Biosensors and Bioelectronics 82 (2016) 255–261

Contents lists available at ScienceDirect

Biosensors and Bioelectronics

journal homepage: www.elsevier.com/locate/bios

Fundamental monomeric biomaterial diagnostics by radio frequency signal analysis

Jae-hoon Ji [a,b], Kyeong-sik Shin [b], Shinill Kang [a], Soo Hyun Lee [b], Ji Yoon Kang [b], Sinyoung Kim [c], Seong Chan Jun [a,*]

[a] School of Mechanical Engineering, Yonsei University, 50 Yonsei-ro, Seodaemun-gu, Seoul 120-749, Republic of Korea
[b] Nano-Bioresearch Center, Korea Institute of Science and Technology, 39-1 Hawolgok Dong, Songbuk Gu, Seoul 136-791, Republic of Korea
[c] Department of Laboratory Medicine, Yonsei University College of Medicine, 50 Yonsei-ro, Seodaemun-gu, Seoul 120-749, Republic of Korea

ARTICLE INFO

Article history:
Received 6 November 2015
Received in revised form
4 March 2016
Accepted 8 March 2016
Available online 9 March 2016

Keywords:
Biosensor
Biomaterial diagnostics
Bio-detection
Label-free
Dielectric relaxation
Radio-frequency

ABSTRACT

We present a new diagnostic technique of fundamental monomeric biomaterials that do not rely on any enzyme or chemical reaction. Instead, it only uses radio frequency (RF) signal analysis. The detection and classification of basic biomaterials, such as glucose and albumin, were demonstrated. The device was designed to generate a strong resonance response with glucose solution and fabricated by simple photolithography with PDMS (Polydimethylsiloxane) well. It even was used to detect the level of glucose in mixtures of glucose and albumin and in human serum, and it operated properly and identified the glucose concentration precisely. It has a detection limit about 100 μM (1.8 mg/dl), and a sensitivity about 58 MHz per 1 mM of glucose and exhibited a good linearity in human blood glucose level. In addition, the intrinsic electrical properties of biomaterials can be investigated by a de-embedding technique and an equivalent circuit analysis. The capacitance of glucose containing samples exhibited bell-shaped Gaussian dispersion spectra around 2.4 GHz. The Albumin solution did not represent a clear dispersion spectra compared to glucose, and the magnitude of resistance and inductance of albumin was higher than that of other samples. Other parameters also represented distinguishable patterns to classify those biomaterials. It leads us to expect future usage of our technique as a pattern-recognizing biosensor.

1. Introduction

Molecular diagnostics have been applied in various fields and applications, such as molecular biology, biosensors, analytical chemistry, and others by using numerous techniques, e.g., electrochemical, optical, and magnetic resonance methods, and so on. Recently, radio frequency (RF, GHz range) electrical signal-based sensors (RESs) have been considered as novel diagnostic tools for biological sensors (Lee et al., 2012, Lee and Yook, 2014; Park et al., 2014a, 2014b; Grenier et al., 2009; Kim et al., 2013; Kim et al., 2015; Yang et al., 2010); chemical sensors (Rauch et al., 2014; Barochi et al., 2011; Rossignol et al., 2013; Tanguy et al., 2015; Potyrailo and Morris, 2007; Zhixin Li et al., 2014); and humidity sensors (Kim et al., 2006; Bernou et al., 2000). This is due to their unique features, such as low cost, low power consumption, and their ability to provide non-invasive and real-time sensing. Another remarkable potential of RESs is their direct sensing capability, which depends on the interaction between the microwaves and materials. According to the dielectric theory, it is widely known that biomolecules exhibit different behaviors of dielectric dispersion at specific frequencies. This has been demonstrated with glucose in the category of monosaccharides (Moran et al., 2000; Fuchs and Kaatze, 2001; Chan et al., 1986; Noel et al., 1996) and albumin, it has been demonstrated in the category of monomer proteins (Grant et al., 1968; Eden et al., 1980; Oncley, 1942). In aqueous solution, albumin represents two distinct dielectric dispersions, i.e., in the moderate frequency region (10^5–10^7 Hz) and in the high frequency region (10^{10}–10^{12} Hz). However, glucose exhibits strong dielectric dispersion in the low-GHz range. Thus, by observing the electrical property, especially capacitance related to dielectric constant, of glucose and albumin subjected to the electrical signal in the low-GHz range, we could utilize this characteristic of glucose and albumin for the detection and classification of glucose and albumin. In the low-GHz range, In the past few decades, various kinds of glucose sensing techniques were developed, including electrochemical (Harper and Anderson, 2010; Oliver et al., 2009), optical (Bahshi et al., 2009), Raman spectroscopy (Olga Lyandres et al., 2008), reverse iontophoresis (Potts et al., 2002), electro-thermal (Park et al., 2014a, 2014b) and field

* Corresponding author.
E-mail addresses: scj@yonsei.ac.kr, jykang@kist.re.kr (S.C. Jun).

http://dx.doi.org/10.1016/j.bios.2016.03.016
0956-5663/

effect transistor-based (Miyahara and Moriizumi, 1985) methods. Each of these methods has its particular advantages and successes to date. However, such methods are not possible without some bulky enzymes, such as glucose oxidase, hexokinase, or glucose-6-phosphate dehydrogenase for more accurate results (Oliver et al., 2009). This is the intrinsic and inevitable prerequisite in these methods. The use of enzymes or even simple chemicals also increases cost and creates production problems. Thus, we expect that the RES, which is a direct detection method for glucose, can slightly ameliorate these drawbacks. Currently, the number of people who have diabetes mellitus caused by imbalances in their glucose levels has increased due to changes in lifestyle and diet (Cowie et al., 2006). Thus, glucose research, especially for the detection and surveillance of glucose, is considered more important now than it was earlier.

Albumin, a non-glycosylated, multifunctional, negatively-charged plasma protein, is a fundamental protein in humans (He and Carter, 1992). It comprises 50% of the total protein in the plasma, making it the most abundant protein and monomeric proteins in human plasma. One of its main functions in the human body is to regulate the osmotic pressure of blood. It has hydrophobic binding sites in its center and hydrophilic binding ligands in its outer parts (Farrugia et al., 2010). Due to its abundance in mono-protein of albumin, it has been studied extensively in protein diagnostics, immunology, and other areas of research in which antigen-antibody reactions are used (Theodore, 1985; Doumas et al., 1971).

Even albumin and glucose are fundamental biomaterials, and it is worthwhile to investigate them due to their importance to human life, it is not easy to examine them at once. In human bloods or any other real samples, it is inevitable that glucose and albumin exist as a mixture, and we must purify the samples to obtain the respective materials. Thus, it is extremely difficult to examine the properties of target molecules in the mixed condition without any supporting specific reaction for detecting them. In this regard, as mentioned previously, the distinct dielectric behavior of the glucose and albumin merits attention for direct sensing. However, since the glucose and albumin exhibited their own unique properties in response to RF signals, simply investigating the dielectric properties of various bio-samples with a device, such as a dielectric spectrometer, is not sufficient for use as a biosensor. The amount and concentration of the samples required for sensing are much too high to be used as a sensor application, and the work required in using a dielectric spectrometer is quite cumbersome. To solve these problems, we constructed a device that operated as a kind of reflection notch filter in the RF range and exhibited clear resonance of the inductance from the electrode and the capacitance from the sample (Matthaei et al., 1980). The electrode was designed to generate electrical resonance with glucose in a few milli-molar range, which corresponds to the concentration range in human blood. Compared to the previous report of Wang's group (Kim et al., 2015) and our previous work (Park et al., 2014b), this work has some advantages. First, this work has an improvement about detecting limit. Limit of detections (LODs) of the report of Wang's group and our previous work are 8.01 mg/dl (0.45 mM), 18 mg/dl (1 mM), respectively. Additionally, the electrical properties of the samples were extracted from the de-embedding technique and the analysis of equivalent circuit.

RF signals were measured easily as a scattering S-parameter that is a power signal. In doing so, we are able to observe the resonance condition very quickly. To gather more a comprehensive understanding of the electrical properties of biomaterials under RF electrical signal and more reliable discrimination between biomaterials, we tried to de-embed the RF signals from the multi-dimensional electrical parameters by using suitable equivalent circuit analysis (Jun et al., 2007). An R-L-C (resistance-inductance-capacitance) circuit model was constructed that could be analyzed freely from the contact resistance and the contact capacitance between the target sample and the electrode to extract the properties of the targets. The various parameters that were obtained by processing the analytical signal yielded more reliable results for instant in-situ sensing, with each parameter exhibiting distinct patterns depending on the contents of the sample, even with mixtures of glucose and albumin. The capacitance of each sample that were well-matched to dielectric theory. Thus, we also expect that the analysis of the various parameters de-embedded by our model has a potential for use recognizing direct patterns using RF signals.

2. Materials and methods

Detailed descriptions of the preparation methods of the samples are provided in the Supporting information S1. A highly resistive ($>4000\ \Omega$/cm) silicon (Si)/silicon oxide (SiO_2, 500 nm oxide layer) substrate was selected in order to minimize the signal loss to the substrate, and then a ground-signal-ground (GSG) electrode pattern was fabricated on the substrate by photolithography. The electrode material consisted of Ti/Au (10/150 nm) that was deposited using e-beam evaporation. In a GSG electrode, two ground electrodes were used as the ground base around the signal (Fig. 1d), and the signal electrodes were two transmission electrodes (with a 3-μm gap that became more narrow (2 μm) at the end of the tip). These electrodes were designed to generate electrical resonance with certain bio-samples (glucose) (Fig. 1e). In addition, to eliminate other unexpected influences on the experiment, a polydimethylsiloxane (PDMS) elastomer well (1.5 mm well in diameter and 3 mm thick) was also deposited on the electrode to facilitate dropping the target solution (6 μl) in an exact position (in the middle of the signal electrode) and creating uniformly-shaped droplets between the signal electrodes. The schematic diagram in Fig. 1b and the photograph of the device in Fig. 1e show the completed device. Fig. 1f shows the equivalent circuit between the two ports of our RES. The RF signals were obtained as S-parameter forms that were measured using a network analyzer (E5071 C, ENA Series Network Analyzer by Agilent Technologies) at −20 dBm. The S-parameter is the relative value of the voltage of the two ports. Generally, a notation such as S_{ab} is used to indicate the S-parameter, where “b” represents the applied incident (input) voltage of the port “b”, and “a” signifies the measured voltage of the port “a”. Thus, S-parameter is composed of 4 parameters: S_{11}, S_{21}, S_{12} and S_{22}. S_{11} and S_{22} demonstrate reflected signals of the device and S_{21} and S_{12} exhibit signals transmitted through the solution and the electrode. Before observing the S-parameters of the samples, the signal to the network analyzer was calibrated using the short-open-load-through standards. After dropping a target solution in the well, the S-parameters were measured and used to determine the contents of the sample and the concentration of the solute. Contingent upon the kind and the concentration of the sample, the samples had diverse effects on the electric field in the RF range. The S-parameter that was obtained was decomposed to interrogate the electrical properties of the sample itself, i.e., the resistance (R), the inductance (L), the capacitance (C), and the contact properties of the sample with electrodes, namely, the contact resistance (R_c), and the contact capacitance (C_c), and the parasitic capacitance (C_{ps}). The decomposition of the S-parameter into electrical parameters was conducted by the de-embedding technique and numerical analysis with an equivalent circuit. Detailed descriptions of the techniques are provided in the next section. Furthermore, the relative signal loss resulting from the absorption by the target solution was also calculated by the following loss equation.

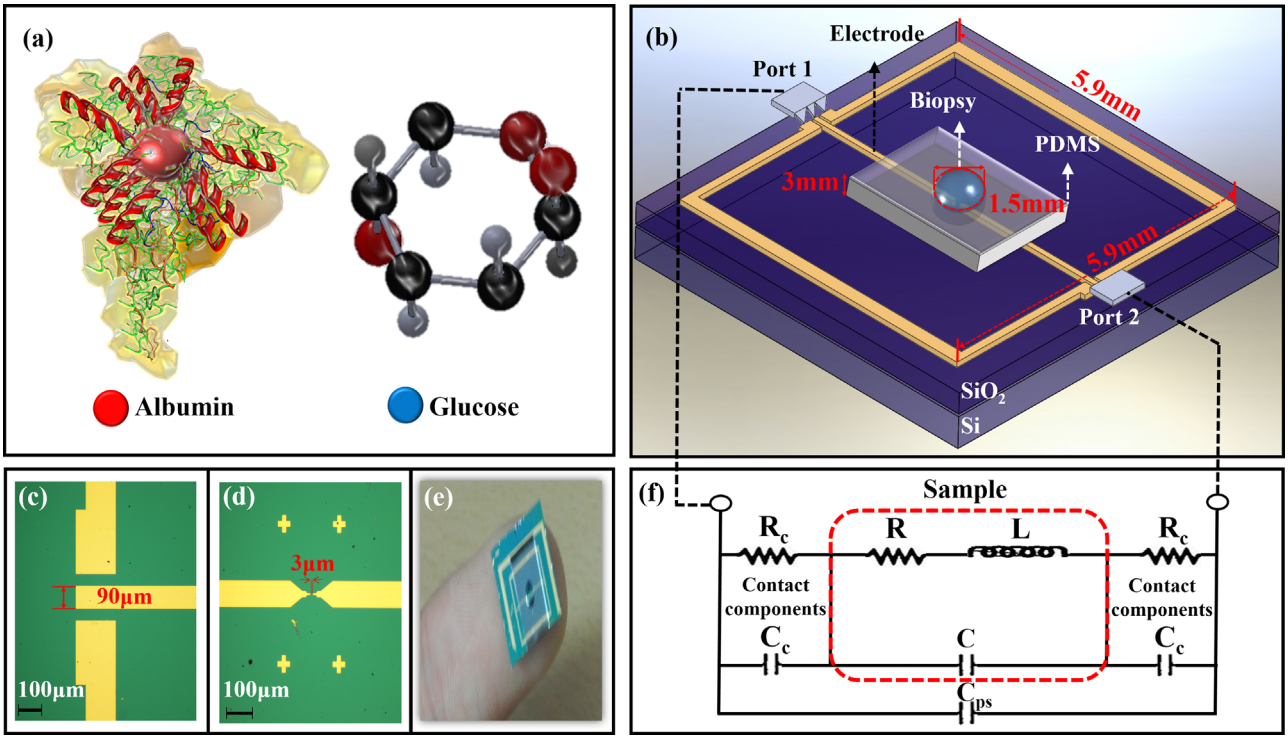

Fig. 1. (a) Virtual images of albumin and glucose. (b) Schematic drawing of the device. (c) Optical microscope image of GSG electrodes that contact with the probe. (d) Optical microscopic image of signal electrodes. (e) Photograph of the device. (f) The equivalent circuit of the device after dropping the sample in the well. It consists of the sample part that includes its R (resistance), L (inductance) and C (capacitance) and the contact parts between the electrodes that include the R_c (contact resistance), C_c (contact capacitance) and the parasitic capacitance of the gap.

$$\text{Loss}=1-[S_{11}]^2-[S_{21}]^2 \quad (1)$$

3. Results and discussion

3.1. Power signals of glucose, albumin solutions, and mixed solutions of glucose and albumin

The reflection parameter (S_{11}) in Fig. 2a shows how much of the signal was reflected to its original port. It is a relative value of the voltage at the port after operation. The device operated well as a reflection notch filter when the sample was Glu. The reflection parameter of Glu decreased sharply after 2.4 GHz, showing a strong resonance dip around 3.6 GHz, which indicated that the signal's power was absorbed mostly near that frequency. However, Alb did not demonstrate any strong band-absorbing behavior in that frequency range. This was due to the unique (and different) dielectric characteristics of Glu and Alb when an AC voltage was applied with a frequency range of 10^8–10^{10} Hz. The detailed description of dielectric theory is discussed in Supporting information S2.

Due to the relaxation coupling with glucose and water, the higher the solution's glucose concentration becomes, the more the dielectric property of the solution is relaxed. In the frequency range of a few GHz, the dielectric dispersion of albumin is located approximately between the 2nd constant region (CR) and 2nd dynamic region (DR), and the dispersion of glucose is located approximately at the 1st DR. The dielectric property of glucose in water changes dynamically above 0.5 GHz (K. Fuchs and Kaatze, 2001). Above this frequency, the imaginary permittivity of Glu places a climax point around about 2.5 GHz and decreases, showing a bell-shaped dispersion. Therefore, the capacitance of the solution between the two ports is altered drastically 0.5–5 GHz. The change of capacitance is discussed in Section 3.3.

The coupling between the capacitance of Glu, which changed dramatically due to its relaxation, and the reactance of the electrode created a strong electrical resonance, as represented by the reflection parameter. It is also important that this resonant tendency be maintained, even in the case of the solution that contains a mixture of glucose and albumin (MGA). All kinds of solutions contained the same concentration of PBS, but only the solution containing glucose exhibited strong resonance. Thus, even it is widely known that ions in solutions could influence the electrical transmission property in the RF range, we could consider that the inclination toward strong resonance originated from the property of glucose. The inset of Fig. 2a shows the transmission parameters of each solution. In this case, the signals of the different solutions did not exhibit clear differences based on the solute. In aqueous condition, the conductivity of the solution is highly depended on the concentration of ion. In our case, the samples had similar concentrations of ions, i.e., mostly phosphate, sodium, potassium, and chloride ions. Therefore, the samples did not have any noticeable difference in conductivity, and they did not have noticeably distinct transmission ability.

Fig. S1 shows the losses of albumin and glucose (see Supporting information). As we predicted previously, the loss level of glucose was much greater than that of albumin due to the dynamic dispersion, and the magnitude of the loss increased in a concentration-dependent manner. The energy toward the opposite port for transmission was dissipated by the dispersion and losses. Additionally, the loss level of PDMS well, relative to the bare electrodes, was far smaller than those of Glu and Alb. We could presume that the most of the electrical signal in RF was dissipated by the sample added to the PDMS well rather than by the well itself. In Fig. 2b, the reflection level of Alb did not show any resonance dip in the frequency range and continuously increased as its concentration increased from 0.5 to 1.5 mM. Since Alb had already experienced its 1st dynamic dispersion at a low frequency and now was situated between the 2nd CR and the 2nd DR, the reflection signal of Alb was quite different from that of Glu and MGA.

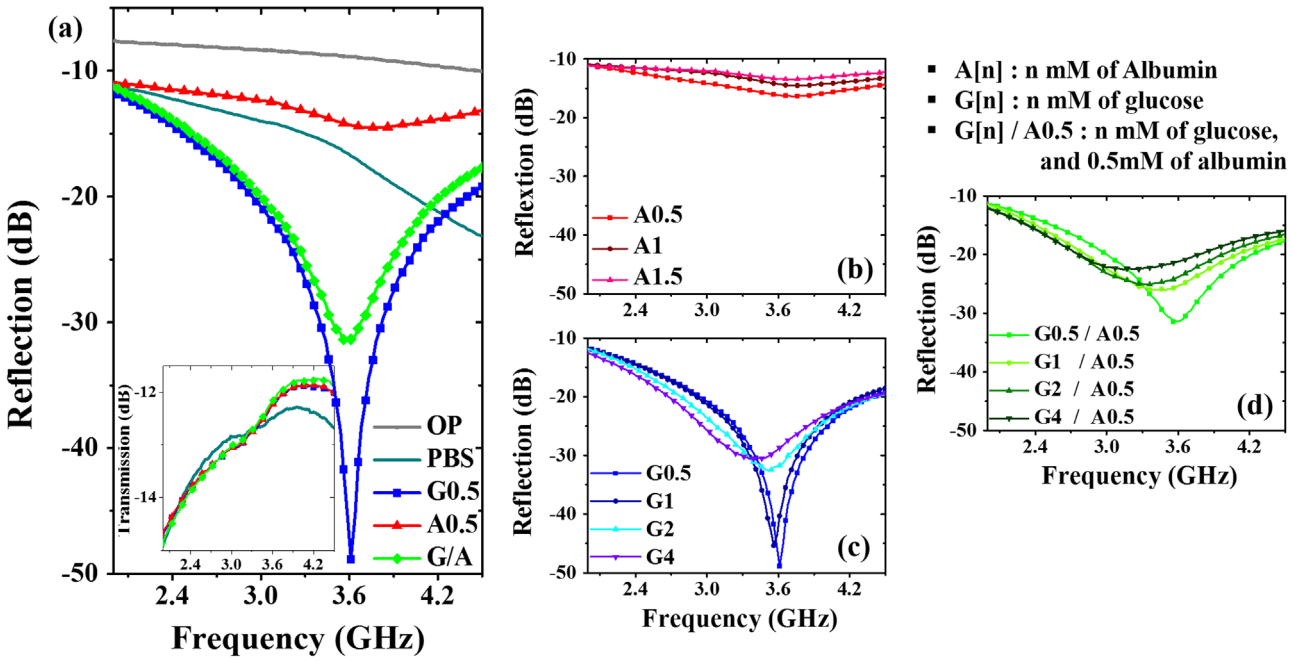

Fig. 2. (a) Reflection parameters (S_{11} of the scattering parameter) of an open sample well (OP) and solutions of PBS, glucose (G0.5: 0.5 mM glucose), albumin (A0.5: 0.5 mM albumin) and mixed solution of glucose and albumin (0.5 mM each of glucose and albumin) for frequencies of 2–4.5 GHz. Reflection parameters of (b) albumin solutions of various concentrations, (c) glucose solutions of various concentrations and (d) solutions with different concentrations of glucose and the same concentration of albumin (0.5 mM). A[n], solution with [n] mM of albumin (n=0.5, 1.0, 1.5 mM); G[n], solution with [n] mM of glucose (n=0.5, 1.0, 2.0, 4.0 mM); G[n]/A, solution with [n] mM of glucose (n=0.5, 1.0, 2.0, 4.0 mM) and 0.5 mM albumin.

Fig. 2c and d exhibit the reflection parameters of Glu for different concentrations of glucose (0.5, 1, 2, and 4 mM) and for MGA solutions that had different levels of glucose and the same concentration of albumin (0.5 mM) that is found in human serum. Although MGA contains both of glucose and albumin, the resonance dip point of Glu and MGA shifted to a lower frequency in the same manner. It indicated that the relaxation time of the solution was getting longer by the combined dynamic relaxation between water and glucose. The detailed values of resonance frequencies are shown in Table 1. In Fig. S2 (see Supporting information), the resonance frequencies of samples, which depend on the concentration of glucose, did as good a job of demonstrating good linearity for both of Glu and MGA as the former technique (n=4, $R^2 > 0.99$, sensitivity of glucose=58 MHz per 1 mM of glucose).

Table 1
Resonance frequency of each solution expressed as a reflection parameter (glucose; mixed solutions of glucose and albumin; albumin solution).

Glucose [mM]	Resonance frequency (GHz)	Glucose [mM] and albumin [0.5 mM]	Resonance frequency (GHz)	Albumin [mM]	Resonance frequency (GHz)
0.5	3.594	0.5	3.572	0.5	None
1	3.565	1	3.497	1	
2	3.505	2	3.362	1.5	
4	3.392	4	3.146		

3.2. Impedance analysis of glucose, albumin solutions, and mixed solutions of glucose and albumin

To obtain the impedance of each solution, the S-parameter of each sample was de-embedded from the S-parameter of open electrodes. (The de-embedding process is discussed in Supporting information S3). The de-embedded S-parameters were analyzed using the equivalent circuit analysis as follows (2):

$$Z(j\omega)=\frac{R+j\omega L}{(j\omega)^2LC+j\omega RC+1}+\frac{2R_c}{1+j\omega R_c C_c} \quad (2)$$

where R, L, and C are the resistance, inductance, and capacitance, respectively; R_c and C_c are the contact resistance and contact capacitance, respectively; and ω is the angular frequency (Yoon et al., 2013). The circuit was designed to consider two main components that affects the electric field. First, the interface between the sample and the electrodes was regarded as a huge electrical barrier to the signal due to the tremendous conductivity difference between gold and water. Second, the impedance of the sample itself was considered as another component that may severely influence the electrical signal. The de-embedding process and the extracting process of electrical properties of the sample ware conducted sequentially by numerical analysis with MATLAB 2012. In Figs. S3a–c (see Supporting information), the impedance level of Alb was located in the highest range, and the impedance of Glu was the lowest. This was because Alb has a greater contact resistance than Glu, and this is explained in detail in Section 3.3. In the case of Glu, the impedance decreased from 1.5 to 2.4 GHz and recovered slightly after 2.4 GHz. However, Alb showed consistent decreases in impedance. In the negative phase of each sample (see Supporting information in Figs. S3d–f), Glus had dip points that originated from the dispersive property of glucose around 2.4 GHz, which was the frequency at which sharp decline and dynamics variation in the reflection parameter began. Glu had a steeper fall and rise at around 2.4 GHz than MGA did, due to the influence of the albumin in MGA. Unlike impedance, the extent order of phase in Glu was reversed after the dip point. Before the dip point, the phase decreased depending on the concentration. However, the Alb did not exhibit any dip points in that frequency region, and the phase increased linearly with the increase in the concentration of albumin without any reversal.

3.3. Extracted multi-dimensional electric properties of each solution

As previously stated, we designed an equivalent circuit that was useful in identifying the properties of the samples. To obtain the properties of a sample, the contact components, which consisted of contact resistance and contact capacitance, were considered due to the huge electrical barriers that are built between the electrode and the sample. The magnitude of contact resistance was much greater than that of the resistance of the samples. Figs. S4a and S4b show that the contact resistances of the solutions that contained glucose also exhibited dip points (see Supporting information). The extracted contact resistance of Glu had a steeper curvature than that of MGA. However, the magnitude of the contact resistance of MGA was similar to that of Alb, rather than that of Glu. Like other parameters, the contact resistance of Alb did not represent a similar tendency to that of the solution that contained glucose.

The extracted contact capacitance (see Supporting information in Figs. S4d–f) also show clear distinctions based on the materials that were tested. The dip points of Glu and MGA were located near 2.4 GHz, and they shifted to lower frequencies as the concentrations increased. On the other hand, MGA showed a blunt fall and rise from the influence of albumin. For MGA, it was noted that the magnitude of the contact components was affected to a greater extent by the albumin, while the glucose influenced the aspect of transition in contact conditions along the frequency range. The dielectric properties of each solution are shown in Fig. 3a–c. The amounts and shapes of the droplets of the solutions were almost uniform due to the assistance of the PDMS well. Thus, we can assume that the capacitance of the solutions was affected only by the dielectric properties of each solution. As we predicted earlier, in Fig. 3a, the capacitance of Glu had a bell-shaped dispersion between 2 and 3 GHz. These results are well matched to the dielectric dispersion spectra of glucose. However, in this frequency range, Alb had a relatively small dispersion compared to Glu and, instead, exhibited only weak dispersion (Fig. 3c). Unlike the small dispersion of Alb, the MGA curves in Fig. 3b had bell-shaped dispersions like those of Glu, and even the bends of the curves were lower than those of Glu. From the capacitance dispersion spectra of Glu, we estimated the combined relaxation times of glucose and water. According to the dielectric theory, the dielectric spectrum of Glu can be well explained by a Cole–Cole relaxation model as follows (Cole and Cole, 1941):

$$D_C(f)=\varepsilon(\infty)+\frac{\Delta\varepsilon}{1+i\omega\tau^{(1-h)}} \tag{3}$$

where f is the frequency, D_C denotes the spectral dispersion function of Glu, and $\varepsilon(\infty)$ represents the fully-dispersed permittivity at

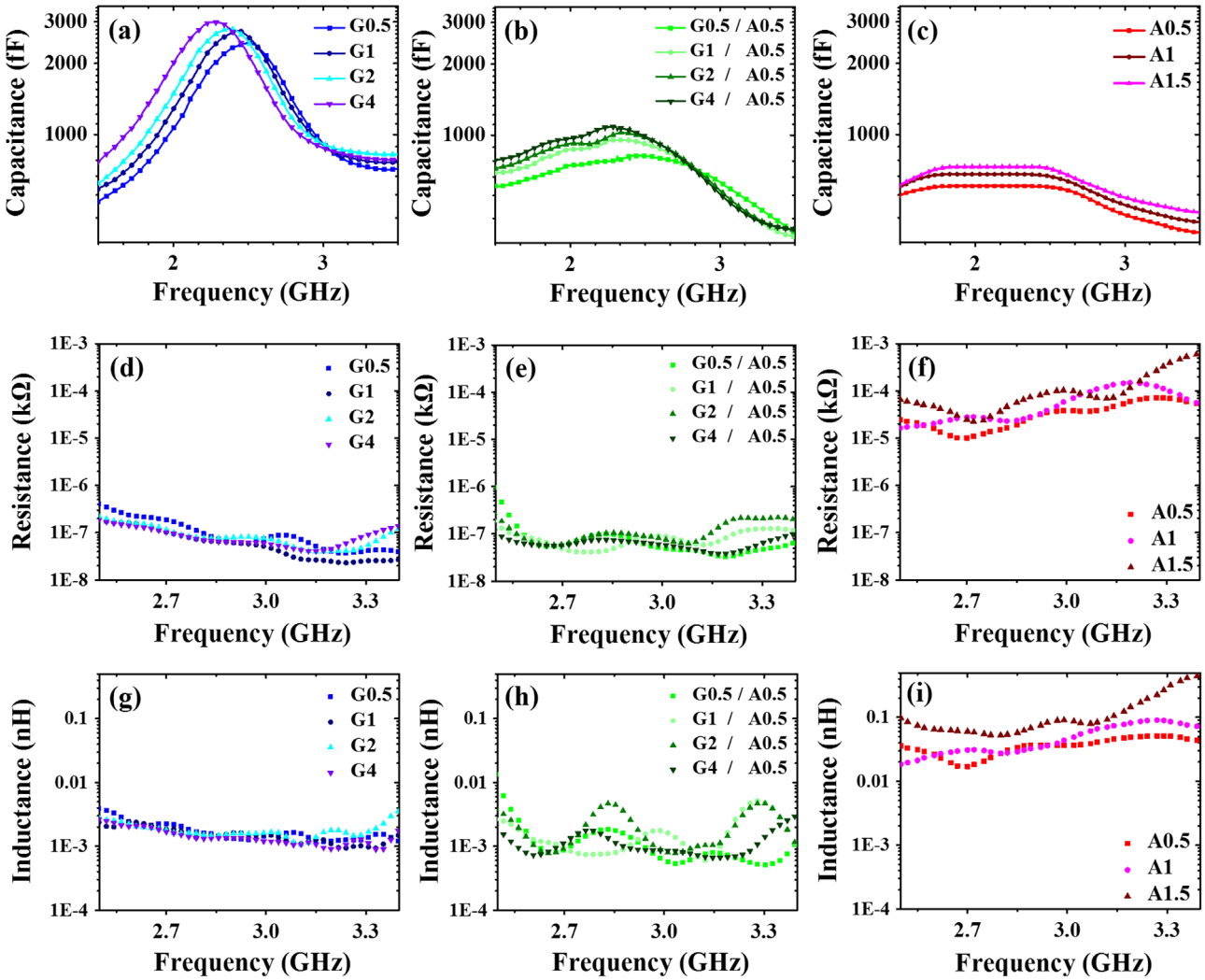

Fig. 3. (a)–(c) Capacitance of glucose solutions, mixed solutions of glucose and albumin, and albumin solutions respectively. (d)–(f) Resistance of glucose solutions, mixed solutions of glucose and albumin, and albumin solutions respectively. (g)–(i) Inductance of glucose solutions, mixed solutions of glucose and albumin, and albumin solutions respectively.

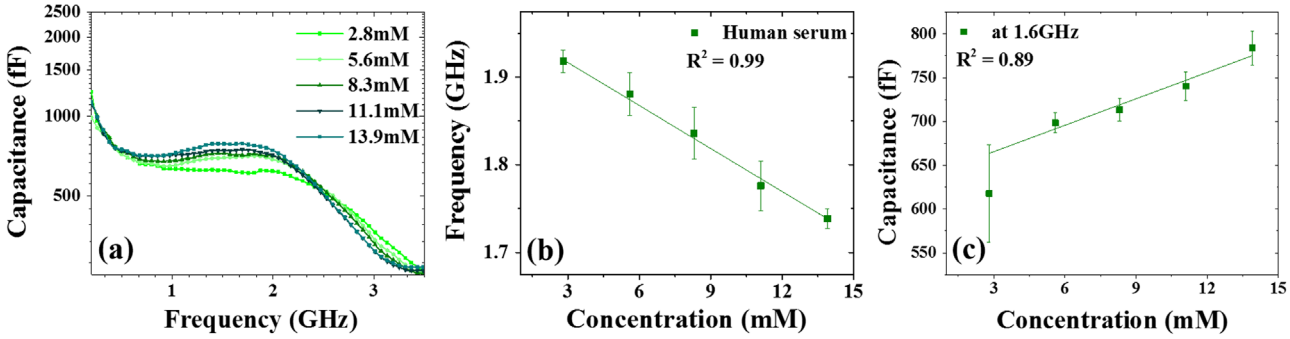

Fig. 4. (a) Extracted capacitance of human serum. (b) Dielectric relaxation frequency of human samples. (c) Capacitance of human samples at 1.6 GHz. 50 mg/dl (2.8 mM)–250 mg/dl (13.9 mM) of glucose (5 samples, the concentration was elevated 2.8 mM per sample).

the high radio frequency that was the previously-mentioned, non-orienting frequency region, such that $\epsilon(\infty)=\lim_{f\to\infty} D_c(f), f < 100$ GHz. In addition, $\Delta\varepsilon$ is the difference in the permittivity between the static condition [$\varepsilon(0)$] and the fully dispersed condition [$\varepsilon(\infty)$], and τ is the dielectric relaxation time of glucose/water. The parameter h is determined by the concentration of the solute in the water, and it is known that h was almost zero in our case (Fuchs and Kaatze, 2001). Thus, the equation of dielectric spectra is simply defined by (4)

$$D_C(f)=\varepsilon(\infty)+\frac{\Delta\varepsilon}{1+i\omega\tau} \quad (4)$$

From the spectra, the relaxation frequency of each solution was obtained successfully. The relaxation time of each condition was also calculated from the simple relationship between frequency and time, i.e., ($f=\frac{1}{2\pi\tau}$). This agrees well with the dielectric theory. The relaxation frequency also shifted linearly, similar to the change of the resonance frequency in reflection parameter in Fig. S5 (see Supporting information, n=4, $R^2>0.98$, sensitivity of glucose=62 MHz per 1 mM of glucose). However, the simplified Eq. (4) was not used directly to interpret the spectra of MGA. In Fig. 3b, the dispersion spectra of MGA are more asymmetric and broader than those of Glu (Havriliak and Negami, 1967). It is considered that the additional interaction of glucose and albumin in the mixed and complexed condition of MGA might influence the dielectric property. Since the hydroxyl groups and other functional groups of albumin that interact easily with glucose are affected by glucose, the non-enzymatic glycation between glucose and albumin might occur. Those additional interactions could influence the dielectric property of MGA. However, without analyzing the detailed parameters, such as broadness and asymmetry of the spectra, utilizing the relaxation frequency and time of MGA obtained directly from the spectra as sensing parameters is still valid. The relaxation frequency and time of MGA that were obtained, depending on the concentration of glucose, were not very different from those of Glu. Additionally, when we consider the dielectric theory, the dominant dielectric relaxation of MGA in GHz operation is not the interaction between albumin and glucose; rather, it is the interaction between glucose and water. Table 2 represents the detailed values of relaxation frequency and time. From the measured capacitance, we also derived the permittivity of the biomaterial. The detailed technique to obtain the permittivity from the capacitance and the result are discussed in Supporting information S4.

Table 2
Relaxation frequency and time of each solution in extracted capacitance. (glucose; mixed solutions of glucose and albumin; albumin solution).

Glucose [mM]	Relaxation frequency and time (GHz/ps)	Glucose [mM] and albumin [0.5 mM]	Relaxation frequency and time (GHz/ps)	Albumin [mM]	Relaxation frequency and time (GHz/ps)
0.5	2.486/64.01	0.5	2.427/65.57	0.5	None
1	2.430/65.50	1	2.397/66.39	1	
2	2.373/67.05	2	2.352/67.66	1.5	
4	2.261/70.38	4	2.277/69.883		

Although Alb did not show powerful, bell-shaped dispersions, the magnitude of capacitance in Alb changed linearly depending on the concentration. The resistance and inductance of Glu and MGA did not exhibit any specific trends that depended on the concentration. However, they did exhibit distinguishable patterns when only albumin was used, and the levels of resistance and inductance for Alb were much greater than those for other conditions. This was thought to be due the fact that the signal in Alb was not affected by the dynamic relaxation of capacitance in the operating frequency, and it seemed that the electrical energy was dissipated as resistive and inductive losses. Specifically, the magnitude of the contact resistance of Glu was about one million times greater than that of the sample itself. The magnitude ratio between the contact and sample resistance of Alb was only about one thousand to one. Additionally, the magnitudes of resistance and inductance magnitude in MGA were similar to those of Glu. It is considered that the electrical energy was dissipated as capacitive losses, when the signal applied to the solution containing glucose.

3.4. Application to human serum

We tried to determine the concentration of glucose in human serum. In human serum samples that contained 50 mg/dl (2.8 mM)–250 mg/dl (13.9 mM) of glucose (five samples, the concentration was elevated at 2.8 mM per sample) were prepared and examined, the same as before. Due to the tremendous diversity of solutes in human serum and the difficulty of control, we even analyzed our multiple parameters for the detection, but only the capacitance showed a meaningful tendency (Fig. 4a). From the above data, the estimated dielectric relaxation frequencies of Glu and MGA when the concentration of glucose was 2.8 mM were 2.36 and 2.32 Hz, respectively, whereas the human serum that contained 2.8 mM of glucose showed dielectric relaxation at 1.92 GHz, far lower than the control cases (n=3, R^2=0.99, sensitivity of glucose=17 MHz per 1 mM of glucose). In Fig. 4c, the capacitance level at 1.6 GHz was also plotted, depending on the concentration (n=3, R^2=0.89, sensitivity of glucose=10 fF per 1 mM of glucose). For glucose with a concentration of 2.8 mM, the level and deviation of capacitance were 618 fF and 55.7 fF, respectively. Thus, LOD and the reliability of the sensing parameter, investigation of the relaxation frequency was more prevalent for sensing the concentration of glucose than observing the level of capacitance. It was seemed that some other unexpected molecules in human serum generated dynamic dielectric relaxation. Other

kinds of monosaccharides, such as fructose and galactose, and small molecules that have hydroxyl groups in blood might affect the dynamic relaxation of the human sample exposed to the RF signal. Although the dielectric relaxation frequency of human serums showed a deviation from the results that were obtained from the control experiments, there was still a tendency for the relaxation frequency to shift to lower frequencies, depending on the increments of glucose concentration.

4. Conclusion

We demonstrated a direct bio-sensing platform based on analyzing the radio-frequency electrical signal of monomeric biomaterial solution, i.e., glucose and albumin. The immediate and direct comparison of biomaterials was conducted by investigating the resonance response and the relaxation frequency of extracted capacitance. For Glu, RES had a LOD of 100 μM and exhibited a reliable linearity (0.99) in the range of glucose concentrations in human blood. Thus, it could be used for diabetes monitoring. It also operated successfully, even for the detection of glucose in mixtures of glucose and albumin and in human serum. On the contrary, RES for Alb did not exhibit a strong resonance reaction about all of the electrical parameters; rather, it only showed magnitude differences in the parameters when it used to observe milli-molar range of albumin. One of the next tasks in developing the RES sensor is a more specific detection within a given category of samples, such as distinguishing glucose and fructose, is another monosaccharide. Then, it is expected that RES would have sufficient potential to be utilized as a pattern recognizing sensor by observing the distinct tendencies of various electrical parameters in each biomaterial within the RF range.

Acknowledgements

This work was partially supported by the Priority Research Centers Program (2009-0093823), the Basic Science Research Program (Grant no. 2013063062), the Korean Government (MSIP) (No. 2015R1A5A1037668) through the National Research Foundation of Korea (NRF) funded by the Ministry of Education, Science and Technology (MEST).

Appendix A. Supporting information

Supplementary data associated with this article can be found in the online version at http://dx.doi.org/10.1016/j.bios.2016.03.016.

References

Bahshi, Lily, Freeman, Ronit, Gill, Ron, Willner., Itamar, 2009. Small 5, 676–680.
Barochi, Guillaume, Rossignol, J.érôme, Bouvet., Marcel, 2011. Sens. Actuators B-Chem. 157, 374–379.
Bernou, Catherine, Rebiere, Dominique, Pistre, Jacques, 2000. Sens. Actuators B-Chem. 68, 88–93.
Chan, R.K., Pathmanathan, K., Johari., G.P., 1986. J. Phys. Chem. 90, 6358–6362.
Cole, K.S., Cole, R.H., 1941. J. Chem. Phys. 9, 341–352.
Cowie, Catherine C., Rust, Keith F., Byrd-Holt, Danita D., Eberhardt, Mark S., Flegal, Katherine M., Engelgau, Michael M., Saydah, Sharon H., Williams, Desmond E., Geiss, Linda S., Gregg, Edward W., 2006. Diabetes Care 29, 1263–1268.
Doumas, Basil T., Watson, W. Ard, Biggs, Homer G., 1971. Clin. Chim. Acta 31, 87–96.
Eden, Joyce, Gascoyen, Peyer R.C., Pethig, Ronald, 1980. J. Chem. Soc. Faraday Trans. 1 76, 426–434.
Farrugia, Albert, 2010. Transfus. Med. Rev. 24, 53–63.
Fuchs, K., Kaatze, U., 2001. J. Phys. Chem. B 105, 2036–2042.
Grant, Edward H., Keefe, Susan E., Takashima, Shiro, 1968. J. Phys. Chem. 72, 4373–4380.
Grenier, Katia, Dubuc, David, Poleni, Paul-Emile, Kumemura, Momoko, Toshiyoshi, Hiroshi, Fujii, Teruo, Fujita, Hiroyuki, 2009. IEEE 57, 12.
Harper, Alice, Anderson, Mark R., 2010. Sensors 10, 8248–8274.
Havriliak, S., Negami, S., 1967. Polymer 8, 161–210.
He, Xiao Min, Carter, Daniel C., 1992. Nature 358, 209–215.
Jun, Seong Chan, Huang, X.M.H., Sungwon Moon, Kim, H. Jin, Hone, James, Jin, Y.W., Kim., J.M., 2007. New J. Phys. 9, 265.
Kim, N.Y., Dhakal, R., Adhikari, K.K., Kim, E.S., Wang., C., 2015. Biosens. Bioelectron. 67, 687–693.
Kim, Sang-Gyu, Lee, Hee-Jo, Lee, Jung-Hyun, Jung, Hyo-Il, Yook, Jong-gwan, 2013. Biosens. Bioelectron. 50, 362–367.
Kim, Yong-Ho, Jang, Kihun, Yoon, Young Joong, Kim., Yong-Jun, 2006. Sens. Actuators B-Chem. 117, 315–322.
Lee, Hee-Jo, Yook, Jong-gwan, 2014. Biosens. Bioelectron. 61, 448–459.
Lee, Hee-Jo, Lee, Jung-Hyun, Moon, Hui-Sung, Jang, Ik-Soon, Choi, Jong-Soon, Yook, Jong-gwan, Jung, Hyo-I.L., 2012. Sens. Actuators B-Chem. 169, 26–31.
Matthaei, G., Jones, E.M.T., Young, L., 1980. Microw**ave** Filters, Impedance-Matching Networks, and Coupling Structures. Artech House, Norwood.
Miyahara, Yuji, Moriizumi, Toyosaka, 1985. Sens. Actuators 7, 1–10.
Moran, Gerald R., Jeffrey, Kenneth R., Thomas, Jason M., Stevens, James R., 2000. Carbohydr. Res. 328, 573–584.
Noel, Timothy R., Parker, Roger, Ring., Stephen G., 1996. Carbohydr. Res. 282, 193–206.
Olga Lyandres, Jonathan M., Yuen, Nilam C., Shah, Richard P., Van Duyne, Joseph, T., WalshJr., T., Glucksberg, Matthew R., 2008. Diabetes Technol. Ther. 10, 257–265.
Oliver, N.S., Toumazou, C., Cass, A.E.G., Johnston., D.G., 2009. Diabetes Med. 26, 197–210.
Oncley, J.L., 1942. Chem. Rev. 30, 433–450.
Park, Hyung Goo, Yoon, Hyong Seo, Ji, Jae-hoon, Sim, Heung Bo, Kim, Jae Hun, Jun, Seong Chan, 2014a. Curr. Appl. Phys. 14, 1553–1556.
Park, Hyunggoo, Yoon, Hyung Seo, Patil, Umakant, Anoop, Rani, Lee, Juho, Lim, Juhwan, Lee, Woonhyoung, Jun, Seong Chan, 2014b. Biosens. Bioelectron. 54, 141–145.
Potts, Russell O., Tamada, Janet A., Tierney., Michael J., 2002. Diabetes Metab. Res. Rev. 18, 49–53.
Potyrailo, Radislav A., Morris, William G., 2007. Anal. Chem. 79, 48–51.
Rauch, Dieter, Kubinski, David, Simon, Ulrich, Moos, Ralf, 2014. Sens. Actuators B-Chem. 205, 88–93.
Rossignol, J., Barochi, G., de Fonseca, B., Brunet, J., Bouvet, M., Pauly, A., Markey., L., 2013. Sens. Actuators B-Chem. 189, 213–216.
Tanguy, Nicolas R., Fiddes, Lindsey K., Yan, Ning, 2015. ACS Appl. Mater. Interfaces 7, 11939–11947.
Theodore Jr., Peters, 1985. Adv. Protein Chem. 37, 161–245.
Yang, Yang, Zhang, Hanqiao, Zhu, Junjie, Wang, Gaoyan, Tzeng, Tzuen-Rong, Xuan, Xiangchun, Huang, Kama, Wang, Pingshan, 2010. Lab Chip 10, 553–555.
Yoon, Hyong Seo, Kim, Whan Kyun, Jung, Young Mo, Cho, Joon Hyong, Kim, D.H., Song, In. Sang, Choi, Jung Han, Baik, Seunghyun, Chan, Seong, 2013. Nanotechnology 24, 015201.
Zhixin, Li, et al., 2014. Sens. Actuators B-Chem. 196, 23–30.